Effects of Milling Conditions on Nano-scale MnFe(P,Si) Particles by Surfactant-assisted High-energy Ball Milling

Thang, N. V.; Van Dijk, N. H.; Brück, E.

DOI
10.1016/j.phpro.2015.12.183

Publication date
2015

Document Version
Final published version

Published in
Physics Procedia

Physics Procedia

Volume 75, 2015, Pages 1104–1111

20th International Conference on Magnetism

Effects of milling conditions on nano-scale MnFe(P,Si) particles by surfactant-assisted high-energy ball milling

N.V. Thang, N.H. van Dijk, E. Brück

Fundamental Aspects of Materials and Energy,
Department of Radiation Science and Technology,
Delft University of Technology, Mekelweg 15, 2629 JB Delft, The Netherlands
V.T.Nguyen-1@tudelft.nl, N.H.vanDijk@tudelft.nl, E.H.Bruck@tudelft.nl

Abstract

The influence of the milling conditions on the nano-scale MnFe(P,Si) particles obtained by surfactant-assisted high-energy ball milling has been investigated by X-ray diffraction (XRD) and magnetic measurements. The presence of surfactant oleic acid prevents the re-welding of crushed particles and enhances the dispersion of nanoparticles in the solvent during the ball milling. The XRD peak intensities decrease and the peaks broaden with increasing milling time, indicating a decrease in grain size. For increasing milling time, the spontaneous magnetization becomes lower and the thermal hysteresis becomes smaller. The surfactant concentration does not have a strong impact on the magnetic properties of the obtained nanoparticles, which is consistent with the X-ray diffraction data showing the same patterns at different surfactant concentrations.

Keywords: Magnetocaloric effect, nano-scale particles, surfactant-assisted high-energy ball milling

1. Introduction

From both fundamental and practical point of view, the study of the magnetocaloric effect (MCE) in magnetic materials is important because it provides information about the magnetic state and the magnetic phase transition of the MCE material under investigation, but the MCE can also be applied in magnetic refrigeration [1]. Until now, most of the research has focused on the preparation of magnetocaloric materials with micro-scale particles.

In this work, we explore the possibility to produce magnetocaloric nanoparticles. The fabrication of nanoparticles of magnetocaloric materials is of interest from both fundamental and application perspectives [2],[3]. Nanosized MCE materials are predicted to show new magnetic properties compared with bulk materials due to a larger surface-to-volume ratio in nanoparticles, which influences both the magnetic and electronic properties [4],[5]. Moreover, magnetocaloric nanoparticles are more desirable than their bulk counterparts for optimal magnetic refrigeration

Selection and peer-review under responsibility of the Scientific Programme Committee of ICM 2015

doi:10.1016/j.phpro.2015.12.183

because the particle size distribution and inter-particle interactions have been shown to broaden ΔS_m over a wide temperature range, thus enhancing refrigeration capacity (RC) [6].

Various top-down and bottom-up methods such as surfactant-assisted high-energy ball-milling [7], mechanical alloying [8], sputtering [9], co-precipitation [10], solid-state reaction [11], and sol-gel [12] have been developed to prepare different nanosized materials. In this work, we have used a surfactant-assisted high-energy ball milling technique (top-down) to synthesize $Mn_{1.25}Fe_{0.7}P_{0.6}Si_{0.4}$ nanoparticles because it is a simple, inexpensive, efficient and promising method for the preparation of magnetocaloric nanomaterials. The surfactant acts as lubricant on the particle surfaces to prevent the re-welding of crushed particles during the ball milling and enhances the dispersion of nanoparticles in a solvent [13],[14],[15].

2. Experimental

$Mn_{1.25}Fe_{0.7}P_{0.6}Si_{0.4}$ nanoparticles have been produced by a two-stage high-energy ball milling (HEBM) using a planetary ball mill (Fritsch Pulverisette) with the grinding bowls (80 ml volume) and balls (10 mm diameter) made of tungsten carbide. Heptane (C_7H_{16}) (99.8% purity) was used as the solvent and oleic acid ($C_{18}H_{34}O_2$) (90%) was used as the surfactant for the second stage of the milling process. In the first stage, $Mn_{1.25}Fe_{0.7}P_{0.6}Si_{0.4}$ samples were prepared by the same protocol as described in Refs [16],[17]: first high-energy ball milling and then solid state reaction. In the second stage, the powder obtained in the first step was ball-milled again in a protective argon gas atmosphere with the presence of organic solvent heptane and surfactant oleic acid for milling times vary from 0 to 10 hours. The amount of surfactant employed was varied from 0% to 30% of the powder weight while keeping the solvent amount constant at 60% of the powder weight. A constant ball-to-powder weight ratio of 10: 1 and a constant rotation speed of 380 rpm are used for all samples. The slurry mixture obtained after milling was then dispersed into heptane solvent by ultrasonic vibration and transferred to centrifugal tubes for removing the excess surfactant and dried in vacuum afterwards.

The crystalline structures of the particles were characterized by a PANalytical X-pert Pro diffractometer using Cu K_α radiation at the room temperature. Magnetic measurements were performed using the Reciprocating Sample Option (RSO) mode in a Superconducting Quantum Interference Device (SQUID) magnetometer (Quantum Design MPMS 5XL). Scanning Electron Microscope (SEM) and Transmission Electron Microscope (TEM) have been used to investigate the particle size and morphology of the samples.

3. Results and discussion

Figure 1. Color of the liquids obtained after milling with and without a surfactant.

To study the function of the surfactant during the ball milling, the samples were prepared by milling with and without the surfactant. Without the surfactant, the heptane remained clear after milling while it changed color from transparent to brown when the surfactant was added to the milling process (see Fig. 1). This indicates that the existence of the surfactant is essential for the dispersion of the nanoparticles in the solvent during the ball milling process.

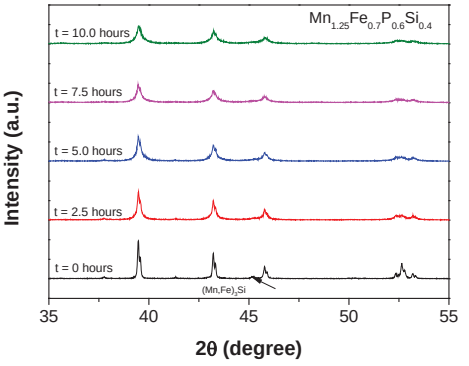

Figure 2. X-ray diffraction patterns measured at room temperature for the $Mn_{1.25}Fe_{0.7}P_{0.6}Si_{0.4}$ samples as a function of the ball milling time.

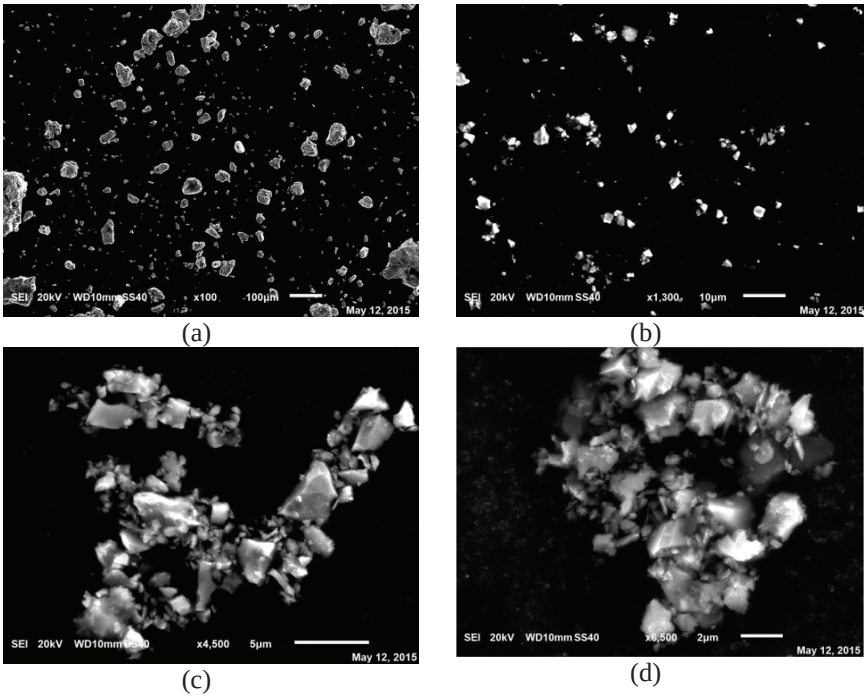

Figure 3. SEM images of $Mn_{1.25}Fe_{0.7}P_{0.6}Si_{0.4}$ compounds obtained before (a) and after milling with the solvent and surfactant for (b): 5.0 hours, (c): 7.5 hours, d: 10.0 hours.

In order to study the effect of the ball milling time on the structural and magnetic properties, the powder obtained in the first step was ball-milled again in a protective argon gas atmosphere with 60 wt.% of heptane and 10 wt.% of oleic acid for 2.5, 5.0, 7.5 and 10.0 hours. The XRD diffraction patterns of the $Mn_{1.25}Fe_{0.7}P_{0.6}Si_{0.4}$ powders obtained before and after milling for different milling times (in the presence of organic solvent heptane and surfactant oleic acid) show that all milled powders exhibit the hexagonal Fe_2P-type structure. In addition, we observe $(Mn,Fe)_3Si$ as an impurity phase (see Fig. 2). As shown in Fig. 2, the XRD peak intensities decrease while the peaks broaden as the milling times increase, indicating a decrease in particle size. Along with the decrease in the particle size, the strains which are induced during the milling process may also contributed to both a decrease in the peak intensity and a broadening of the diffraction peaks [18].

The SEM images of the obtained $Mn_{1.25}Fe_{0.7}P_{0.6}Si_{0.4}$ particles in Fig. 3 show irregular shapes and a wide size distribution. It is clearly seen that the sample before ball milling with the surfactant and solvent has a broad size distribution from 1 to 100 μm, while the samples ball milled with the surfactant and solvent are more homogenous. Hence, surfactant-assisted high-energy ball milling is effective in reducing the particle size by varying the ball milling time.

In Fig. 4 the TEM images are shown of the $Mn_{1.25}Fe_{0.7}P_{0.6}Si_{0.4}$ nanoparticles synthesized by ball milling for different times (2.5, 5.0, 7.5 and 10.0 hours) using oleic acid as the surfactant show that there is a decrease in the particle size, but no significant change in morphology of the nanoparticles for increasing ball milling times. Moreover, it is clearly seen that after centrifuge cleaning there remains surfactant covering the surface of nanoparticles.

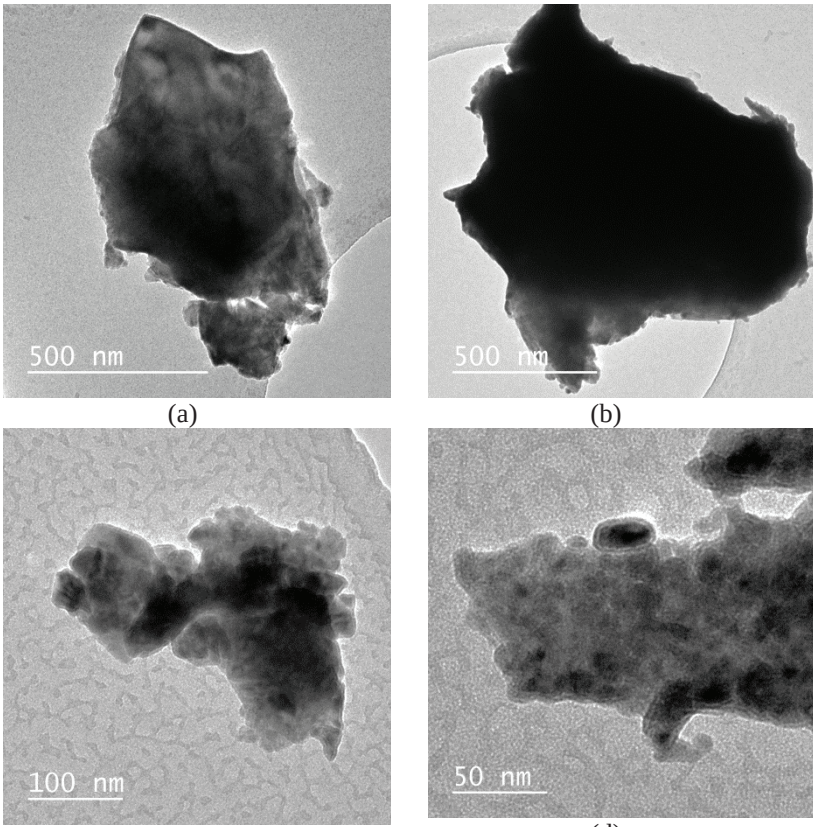

Figure 4. TEM images of the nanoparticles prepared by milling $Mn_{1.25}Fe_{0.7}P_{0.6}Si_{0.4}$ for: (a) 2.5 hours, (b) 5.0 hours, (c) 7.5 hours, (d) 10.0 hours.

Table 1 compares the results of X-ray diffraction and electron microscopy in terms of the average crystallite sizes and the particle sizes, respectively. For X-ray diffraction, the average crystallite size was calculated by applying the Debye-Scherer formula to the maximum intensity (111) peak, which was fitted with the X'Pert High Score Plus software to locate the peak position and the full-width-at-half-maximum (FWHM). It should be noticed that the crystallite size, which is commonly determined by XRD, is the smallest - most likely single crystal in powder form. Particle may be present as a single crystal or an agglomeration of several crystals. Therefore, particle size, which is determined by electron microscopy, is always larger than crystallite size.

Table 1. Variation of grain size for samples before and after ball milling with the surfactant at the different ball milling times.

Milling time (hours)	Particle size from XRD (nm)	Particle size from TEM (μm)
0	272	30-50
2.5	58	-
5	38	2-4
7.5	32	0.5- 2
10	31	0.05 – 0.5

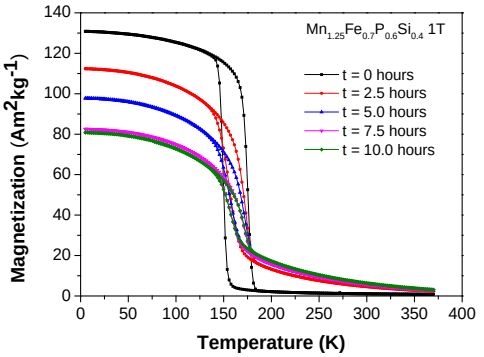

Figure 5. Magnetization of the $Mn_{1.25}Fe_{0.7}P_{0.6}Si_{0.4}$ samples as a function of temperature measured in a magnetic field of 1 T upon heating and cooling.

The temperature dependence of the magnetization for $Mn_{1.25}Fe_{0.7}P_{0.6}Si_{0.4}$ compounds obtained before and after milling with the solvent and surfactant for different milling times is shown in Fig. 5. As can be clearly seen, the *M-T* curve of the $Mn_{1.25}Fe_{0.7}P_{0.6}Si_{0.4}$ powders obtained before ball milling with surfactant and solvent shows a very sharp ferromagnetic to paramagnetic transition and a broad thermal hysteresis, confirming the first-order nature of this transition. When the $Mn_{1.25}Fe_{0.7}P_{0.6}Si_{0.4}$ compounds were milled in heptane with 10 wt.% of oleic acid, the spontaneous magnetization becomes lower, while the thermal hysteresis becomes smaller for increasing milling times. This may be due to (i) a larger contribution of the surface states while the particle size decreases [19],[20] or (ii) the remaining surfactant covering on the surface of nanoparticles, which may lead to an error in the sample mass. The amount of surfactant used is 10% of the powder weight, which causes the potential error in weight. It should be noticed that the structural and magnetic properties of samples milled for 7.5 and 10.0 hours are similar. In other words, the increase in the ball milling time above 7.5 hours does not significantly affect the average particle size of the samples.

Fig. 6 shows the magnetic field dependence of the magnetization of the $Mn_{1.25}Fe_{0.7}P_{0.6}Si_{0.4}$ samples before and after the second ball milling for 2.5, 5.0, 7.5 and 10.0 hours at 5 K. The saturation magnetization decreases with the decrease in the particle size caused by the increase in the ball milling time. As the particle size decreases, atoms near the particle surface may have another electron configuration than internal atoms due to the different chemical and magnetic structures of internal core part and surface shell part of the nano-sized particle [21]. This may lead to a decrease in the exchange interaction for decreasing particle sizes.

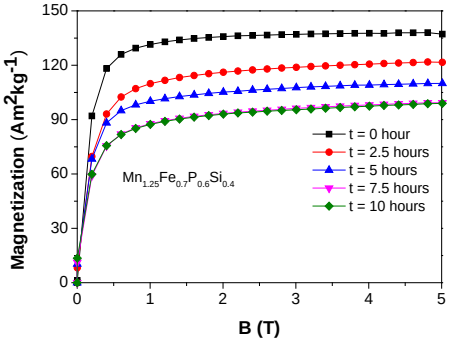

Figure 6. Field dependence of the magnetization of $Mn_{1.25}Fe_{0.7}P_{0.6}Si_{0.4}$ samples measured at 5 K.

Compared to bulk $Mn_{1.25}Fe_{0.7}P_{0.6}Si_{0.4}$ prepared in the first stage, which has $|\Delta S_m| \approx 8$ $Jkg^{-1}K^{-1}$ for a field change of 1 T, we found that the MCE of the $Mn_{1.25}Fe_{0.7}P_{0.6}Si_{0.4}$ powders milled for 10 hours with the solvent and surfactant the first-order transition was smaller ($|\Delta S_m| < 2$ $Jkg^{-1}K^{-1}$) (see Fig. 7). This may be due to the decrease in saturation magnetization caused by the decrease in particle size.

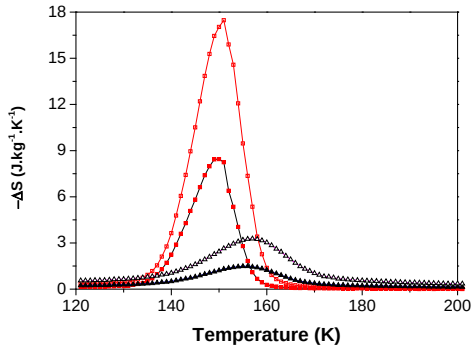

Figure 7. Isothermal magnetic entropy change of $Mn_{1.25}Fe_{0.7}P_{0.6}Si_{0.4}$ samples before (red squares) and after 10 hours second ball milling (black triangles) for a field change of 1 T (for filled symbols) and 2 T (open symbols).

Along with the milling time, the effect of the surfactant concentration has also been studied. The XRD diffraction patterns of $Mn_{1.25}Fe_{0.7}P_{0.6}Si_{0.4}$ powders shown in Fig. 8.a are more or less the same for increasing surfactant concentrations, indicating that the surfactant concentration does not have a strong impact on the structural properties. This is consistent with its effect on the magnetic properties of the obtained nano-scale particles.

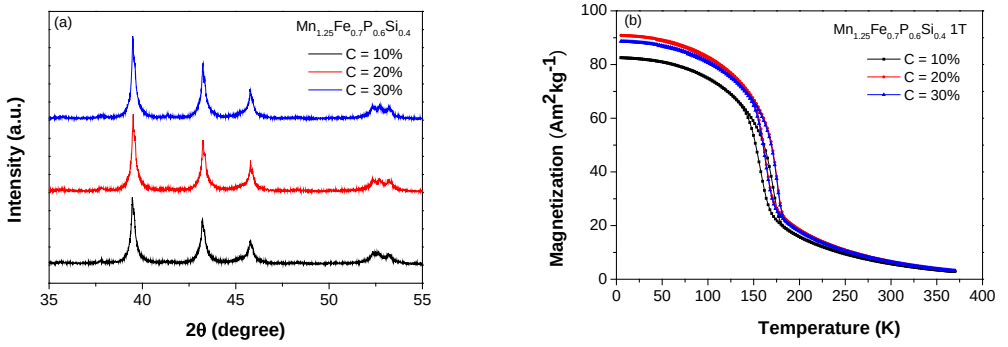

Figure 8. The XRD patterns measured at room temperature (a) and the temperature dependence of the magnetization in a field of 1 T upon heating and cooling (b) for $Mn_{1.25}Fe_{0.7}P_{0.6}Si_{0.4}$ samples obtained after 7.5 hours milling with different surfactant concentrations.

4. Conclusion

Magnetocaloric nanoparticles based on the Fe_2P system have been successfully prepared by surfactant-assisted high-energy ball milling. The influence of the milling parameters such as the ball milling time and surfactant concentration on the structural and magnetic properties of nano-scale $Mn_{1.25}Fe_{0.7}P_{0.6}Si_{0.4}$ particles obtained by surfactant-assisted high-energy ball milling has been investigated. While the surfactant concentration does not significantly affect both the structural and magnetic properties, the increase in the ball milling time leads to a decrease in particle size as well as the magnetocaloric effect.

Acknowledgments

The authors would like to thank A. J. E. Lefering for his technical assistance. This work is funded by the Foundation for Fundamental Research on Matter (FOM) and BASF New Business.

References

[1] A. M. Tishin and Y. I. Spichkin, “Recent progress in magnetocaloric effect: Mechanisms and potential applications,” *International Journal of Refrigeration*, vol. 37, pp. 223–229, Jan. 2014.

[2] J. Gass, H. Srikanth, N. Kislov, S. S. Srinivasan, and Y. Emirov, “Magnetization and magnetocaloric effect in ball-milled zinc ferrite powder,” *Journal of Applied Physics*, vol. 103, no. 7, p. 07B309, 2008.

[3] Q. A. Pankhurst, J. Connolly, S. K. Jones, and J. Dobson, “Applications of magnetic nanoparticles in biomedicine,” vol. 36, 2003.

[4] M. E. Mchenry, “Nano-scale materials development for future,” vol. 48, 2000.

[5] V. Franco, K. R. Pirota, V. M. Prida, A. M. J. C. Neto, A. Conde, M. Knobel, B. Hernando, and M. Vazquez, “Tailoring of magnetocaloric response in nanostructured materials: Role of anisotropy,” *Physical Review B*, vol. 77, no. 10, p. 104434, Mar. 2008.

[6] P. Gorria, P. Álvarez, J. S. Marcos, J. L. Sánchez Llamazares, M. J. Pérez, and J. a. Blanco, "Crystal structure, magnetocaloric effect and magnetovolume anomalies in nanostructured Pr_2Fe_{17}," *Acta Materialia*, vol. 57, no. 6, pp. 1724–1733, Apr. 2009.

[7] V. M. Chakka, B. Altuncevahir, Z. Q. Jin, Y. Li, and J. P. Liu, "Magnetic nanoparticles produced by surfactant-assisted ball milling," *Journal of Applied Physics*, vol. 99, no. 8, p. 08E912, 2006.

[8] a. Hajalilou, M. Hashim, R. Ebrahimi-Kahrizsangi, H. Mohamed Kamari, and S. Kanagesan, "Parametric optimization of $NiFe_2O_4$ nanoparticles synthesized by mechanical alloying," *Materials Science-Poland*, vol. 32, no. 2, pp. 281–291, Jan. 2014.

[9] P. Shah and a. Gavrin, "Synthesis of nanoparticles using high-pressure sputtering for magnetic domain imaging," *Journal of Magnetism and Magnetic Materials*, vol. 301, no. 1, pp. 118–123, Jun. 2006.

[10] K. Petcharoen and a. Sirivat, "Synthesis and characterization of magnetite nanoparticles via the chemical co-precipitation method," *Materials Science and Engineering: B*, vol. 177, no. 5, pp. 421–427, Mar. 2012.

[11] A. Ceylan, S. Ozcan, C. Ni, and S. Ismat Shah, "Solid state reaction synthesis of $NiFe_2O_4$ nanoparticles," *Journal of Magnetism and Magnetic Materials*, vol. 320, no. 6, pp. 857–863, Mar. 2008.

[12] D. Chen and X. He, "Synthesis of nickel ferrite nanoparticles by sol-gel method," vol. 36, pp. 1369–1377, 2001.

[13] Y. Wang, Y. Li, C. Rong, and J. P. Liu, "Sm-Co hard magnetic nanoparticles prepared by surfactant-assisted ball milling.," *Nanotechnology*, vol. 18, no. 46, p. 465701, Nov. 2007.

[14] S. K. Pal, L. Schultz, and O. Gutfleisch, "Effect of milling parameters on $SmCo_5$ nanoflakes prepared by surfactant-assisted high energy ball milling," *Journal of Applied Physics*, vol. 113, no. 1, p. 013913, 2013.

[15] Y. Shen, M. Q. Huang, a. K. Higgins, S. Liu, J. C. Horwath, and C. H. Chen, "Preparation of $PrCo_5$ bulk magnets using nanograin powders made by surfactant-assisted high energy milling," *Journal of Applied Physics*, vol. 107, no. 9, p. 09A722, 2010.

[16] N. H. Dung, L. Zhang, Z. Q. Ou, L. Zhao, L. van Eijck, a. M. Mulders, M. Avdeev, E. Suard, N. H. van Dijk, and E. Brück, "High/low-moment phase transition in hexagonal Mn-Fe-P-Si compounds," *Physical Review B*, vol. 86, no. 4, p. 045134, Jul. 2012.

[17] F. Guillou, G. Porcari, H. Yibole, N. van Dijk, and E. Brück, "Taming the first-order transition in giant magnetocaloric materials.," *Advanced materials (Deerfield Beach, Fla.)*, vol. 26, no. 17, pp. 2671–5, 2615, May 2014.

[18] M. Yue, Y. P. Wang, N. Poudyal, C. B. Rong, and J. P. Liu, "Preparation of Nd–Fe–B nanoparticles by surfactant-assisted ball milling technique," *Journal of Applied Physics*, vol. 105, no. 7, p. 07A708, 2009.

[19] W. Tang, W. J. Lu, X. Luo, B. S. Wang, X. B. Zhu, W. H. Song, Z. R. Yang, and Y. P. Sun, "Size-induced changes of structural, magnetic and magnetocaloric properties of $La_{0.7}Ca_{0.2}Ba_{0.1}MnO_3$," *Physica B: Condensed Matter*, vol. 405, no. 12, pp. 2733–2741, Jun. 2010.

[20] M. Zhang, Z. Zi, Q. Liu, P. Zhang, X. Tang, J. Yang, X. Zhu, Y. Sun, and J. Dai, "Size effects on magnetic properties of $Ni_{0.5}Zn_{0.5}Fe_2O_4$ prepared by Sol-Gel method," vol. 2013, 2013.

[21] D. H. Han, J. P. Wang, and H. L. Luo, "Crystallite size effect on saturation magnetization of fine ferrimagnetic particles," *Journal of Magnetism and Magnetic Materials*, vol. 136, pp. 176–182, 1994.